Epilepsia. Author manuscript; available in PMC 2016 June 02.

Published in final edited form as:
Epilepsia. 2013 April ; 54(4): 605–615. doi:10.1111/epi.12133.

Seizure-like discharges induced by 4-aminopyridine in the olfactory system of the in vitro isolated guinea pig brain

Laura Uva[*], **Federica Trombin**[*], **Giovanni Carriero**[*], **Massimo Avoli**[†], and **Marco de Curtis**[*]

[*]Unit of Experimental Epileptology and Neurophysiology, Fondazione Istituto Neurologico Carlo Besta, Milan, Italy

[†]Departments of Neurology, Neurosurgery, Physiology, Montreal Neurological Institute, McGill University, Montréal, Quebec, Canada

Summary

Purpose—The study of the interactions leading to network- or region-specific propagation of seizures is crucial to understand ictogenesis. We have recently found that systemic (arterial) application of the potassium channel blocker, 4-aminopyridine (4AP), induces different and independent seizure activities in olfactory and in limbic structures. Here, we have characterized the network and cellular features that support 4AP-induced seizure-like events in the olfactory cortex.

Methods—Simultaneous extracellular recordings were performed from the piriform cortex, the entorhinal cortex, the olfactory tubercle, and the amygdala of the in vitro isolated guinea pig brain preparation. Intracellular, sharp electrode recordings were obtained from neurons of different layers of the region of ictal onset, the piriform cortex. Seizure-like discharges were induced by both arterial perfusion and local intracortical injections of 4AP.

Key Findings—Arterial application of 4AP induces independent seizure activities in limbic and olfactory cortices. Both local applications of 4AP and cortico-cortical disconnections demonstrated that region-specific seizure-like events initiated in the primary olfactory cortex and propagate to anatomically related areas. Seizures induced by arterial administration of 4-AP are preceded by runs of fast activity at circa 30–40 Hz and are independently generated in the hemispheres. Simultaneous extracellular and intracellular recordings in the piriform cortex revealed that the onset of seizure correlates with (1) a gradual amplitude increase of fast activity runs, (2) a large intracellular depolarization with action potential firing of superficial layer

Address correspondence to Marco de Curtis, Unit of Experimental Neurophysiology and Epileptology, Fondazione Istituto Neurologico, Milano, Italy. decurtis@istituto-besta.it.

Disclosure

None of the authors has conflicts of interest to disclose. We confirm that we have read the Journal's position on issues involved in ethical publication and affirm that this report is consistent with those guidelines.

Supporting Information

Additional Supporting Information may be found in the online version of this article:

Figure S1. (A) Distribution of experiments showing activity exclusively in the olfactory region (empty column), in the limbic region (black column), or in both structures with a different sequence of activation: PC earlier than m-EC (dark gray column) and m-EC earlier than PC (light gray column). (B) In the early PC onset experiments (on the left; dark gray), time delays measured between the onset of the last SLEs recorded in PC before the m-EC seizure onset are shown. The right panel illustrates early m-EC onset experiments (light gray). Time delays measured between m-EC seizure onset and the SLE onset in PC are reported.

neurons, and (3) no firing in a subpopulation of deep layers neurons. During the ictal event, neuronal firing was abolished for 10–30 s in all neurons and gradually restored and synchronized before seizure termination.

Significance—Our data show that olfactory neuronal networks sustain the generation of seizure-like activities that are independent from those observed in adjacent and connected limbic cortex regions. The data support the concept that functionally and anatomically hard-wired networks generate region-specific seizure patterns that could be substrates for system epilepsy.

Keywords

Epileptic network; Piriform cortex; System epilepsy

The current debate on the classification of seizures and epilepsies introduced the concept of epileptic networks that define focal epileptiform activities (Berg et al., 2010). The term epileptic network extends the notion of epileptic focus and introduces the idea that enhanced excitability within ensemble of strongly interconnected neurons/networks may promote the generation of region-specific synchronous pathologic discharges. This hypothesis has led to the proposition that some forms of idiopathic (and even acquired) epilepsy may represent a specific network dysfunction, due to enduring propensity of the network/system itself as a whole to generate seizures (Avanzini et al., 2012). The existence of predetermined functional network substrates supporting the generation of synchronous activity patterns may represent one of the prerequisites for the definition of system or network epilepsy.

Studies in a number of animal models of generalized epilepsy demonstrated that specific patterns of epileptiform discharges entrain the thalamocortical system (Gloor & Fariello, 1988; Danober et al., 1998; van Luijtelaar & Sitnikova, 2006; Leresche et al., 2012). The hippocampal-parahippocampal region represents another cortical system that is activated as a whole in models of temporal lobe epilepsy and limbic seizures (Avoli et al., 2002; Uva et al., 2005; McIntyre & Gilby, 2008). To gain more information about the cellular and network determinants of seizure generation in these areas, detailed in vitro studies were performed on brain tissue slices. In vitro slices, however, do not allow for an extensive and thorough analysis of network activities, because of the obvious limitations of the preparation itself. Isolated en block brain preparations (de Curtis et al., 1994; Luhmann et al., 2000; Khalilov et al., 2003; Uva et al., 2005) could be better suited for studying the propensity of extended, interconnected cortical regions to generate seizure-like events. We have previously reported that coexisting, but regionally independent, seizure patterns can be induced in brains of guinea pigs maintained in vitro by arterial perfusion by acute pharmacologic manipulations with proepileptic drugs (de Curtis et al., 1994; Uva et al., 2005). Moreover, in Carriero et al. (2010) we have recently demonstrated that in the presence of the potassium channel blocker 4-aminopyridine (4AP; Llinas et al., 1976; Avoli & Perreault, 1987; Perreault & Avoli, 1991), the olfactory cortices and the hippocampal-parahippocampal regions generate independent seizure-like discharges that do not reciprocally interact (Carriero et al., 2010), despite the anatomic and functional connections, and that show a completely different seizure pattern. We extend here the study of ictal discharges recorded in the olfactory system, which is known to be a seizure-prone region (Piredda & Gale, 1985), in this model of ictogenesis, to verify whether this region can be considered as a network

system for seizure generation and to unveil the network and cellular mechanisms that sustain this peculiar activity.

Methods

Experiments were performed on brains isolated from young adult guinea pigs (150–200 g weight; Charles River Laboratories, Calco, Italy). Animals were sacrificed with an intraperitoneal dose of sodium thiopental (125 mg/kg; Farmotal, Pharmacia, Milan, Italy). Three minutes after the paw pinch reflex was extinguished, an intracardiac perfusion with cold saline solution (composition below) was performed to cool brain temperature and to remove blood cells. The brain was isolated according to the previously described protocol (Muhlethaler et al., 1993; de Curtis et al., 1998) and was positioned in an incubation chamber. A polyethylene cannula was inserted in the basilar artery within 2 min to restore brain perfusion via a peristaltic pump (Minipulse 3; Middleton, WI, U.S.A.). The composition of the perfused carboxygenated (95% O_2/5% CO_2) solution was: 126 mM NaCl, 3 mM KCl, 1.2 mM KH_2PO_4, 1.3 mM $MgSO_4$, 2.4 mM $CaCl_2$, 26 mM $NaHCO_3$, 15 mM glucose, 2.1 mM HEPES and 3% dextran MW 70,000 (pH 7.3). The above procedure was performed at 15°C and brain temperature was slowly raised to 32°C via a temperature controller (PTC 10; NPI, Tamm, Germany) before starting the electrophysiologic experiment.

Experimental procedures were conducted in accordance with ethically approved institutional guidelines, in compliance with National and International laws and animal care policies (EEC Council Directive 86/609, OJ L 358, 1, December 12, 1987).

Extracellular recordings were performed with 5–8 μm tip glass micropipettes filled with 0.9% NaCl (5–10 MΩ resistance). Electrodes were positioned in brain structures using surface reference points under direct visual control with a stereoscopic microscope. Responses evoked by stimulation of the lateral olfactory tract (LOT) through an isolation unit driven by a pulse generator (Telefactor S88; Grass, Warwick, RI, U.S.A.) were recorded to test the viability of the preparation during the experiment (Biella & de Curtis, 2000; Biella et al., 2003). Extracellular signals fed to a multichannel differential amplifier (Biomedical Engineering, Thornwood, NY, U.S.A.) were acquired either with a 1 Hz high pass filter or in direct current. Selective band-pass filters were applied to traces when mean frequency content of seizure-like events (SLE) was calculated. Because extracellular signals recorded during fast runs (FRs) and SLEs in piriform cortex (PC) is nonstationary, for the frequency content analysis and time-frequency representation we used short-time-Fourier-transform (STFT) with a Hanning window. The length of the sliding window was set accordingly to the length of the analyzed trace with 1/4 overlap. An average of the frequency content of each phase has been also computed selecting properly the corresponding portion of the signals and applying fast Fourier transform (FFT) algorithm.

Intracellular recordings from neurons in different layers of the anterior PC were performed using glass micropipettes filled with 2 M potassium acetate and 2% biocytin (input resistance 60–120 MΩ). Signals were amplified with a bridge-circuit amplifier (Neuro Data Instruments, New York, NY, U.S.A.). At the end of the recording, cells were injected via the

recording electrode with biocytin. Brains were fixed in 4% paraformaldehyde and cut into 75-μm–thick coronal slices by vibratome. The tissue was then reacted with a standard horseradish peroxidase protocol (ABC kit; Vector Laboratories, Burlingame, CA, U.S.A.), and cell morphology was identified on sections counter-stained with thionine to identify the layers of the cortex.

Amplified neurophysiologic signals were digitized at 3 kHz sampling rate via an AT-MIO-64E3 National A/D Board (National Instruments, Assago, Italy) and were analyzed with custom-made software developed in our lab by Vadym Gnatkovsky (ELPHO). Each cell was characterized by its resting membrane potential (V_{rest}) input resistance, firing threshold, and action potential amplitude. In addition, values of membrane depolarization were evaluated during the progression of fast runs and seizure-like events. All values were expressed as average ± standard deviation (SD). One-way analysis of variance (ANOVA) statistical analysis was performed to compare the mean values of membrane potentials during different phases of the activity. Tukey post hoc test (power = 0.05) was also performed to compare each single group mean versus all the other groups.

To define the depth of the recorded neurons we measured the distance from the pial surface of the location at which the impalement was performed. Piriform cortex neurons were electrophysiologically characterized by considering the delay of the action potential evoked after stimulation of LOT. Spikes riding on either monosynaptic or disynaptic excitatory postsynaptic potentials (EPSPs) are typical of II layer and III layer cells, respectively (Satou et al., 1983). Eight neurons were also morphologically reconstructed after biocytin injection and their depth position was histologically confirmed on thionine-counterstained coronal sections.

Epileptiform activities were induced by 4-min arterial application of the potassium channel blocker, 4-aminopyridine (4AP; Fluka, Milan, Italy; 50 μM; Llinas et al., 1976; Avoli & Perreault, 1987). In addition, local applications of 4AP (2–5 mM) were performed through a glass injection pipette (tip diameter 10 μm) connected to a pressure-ejection system (Picospritzer II; Parker Instrumentation, Cleveland, OH, U.S.A.).

Results

As previously reported (Carriero et al., 2010) arterial application of 4AP (50 μM) induced independent seizure-like activities in both the olfactory region and the limbic region (inclusive of amygdala, hippocampus, and para-hippocampal cortices) of the in vitro isolated guinea pig brain. This is illustrated in Fig. 1. Simultaneous recordings in the PC, lateral entorhinal cortex (l-EC), hippocampal CA1 field (hipp), and medial entorhinal cortex (m-EC) demonstrated the occurrence of typical limbic seizures in CA1/m-EC, characterized by fast activity at onset followed by irregular spiking and rhythmic bursting (see also Uva et al., 2005; Gnatkovsky et al., 2008; Carriero et al., 2010). In the PC, we observed runs of fast activity (fast runs [FRs]; arrows) that progressively became more robust and ultimately generated all-or-none seizure-like events (SLE; arrowheads). Piriform cortex SLEs propagated to the l-EC, where limbic seizures were also observed (Fig. 1; see Uva et al., 2005). We analyzed experiments in which recordings in the olfactory region and limbic

region were simultaneously performed. In 23 experiments, exclusive activation of either olfactory (n = 18) or limbic regions (n = 5) was observed, suggesting the independency of the two epileptiform generators (Fig. S1A). In 19 experiments both regions were activated, with a first discharge of either PC (n = 11) or m-EC (n = 8). Figure S1B shows that seizure onsets in the two regions have highly variable delays (up to 150 s) and therefore are not time locked, suggesting independence of generation. Moreover, the number of the PC SLEs preceding the m-EC seizure onset and the SLE phase during which the m-EC seizure started were also highly variable. In only 3 of 42 cases the spike activity in PC (phase III, see below) propagated to m-EC possibly entraining subsequent epileptiform activity in m-EC.

First, we characterized the spatial distribution of the synchronous pattern recorded in the olfactory area. We performed simultaneous extracellular recordings at several sites along the rostrocaudal axis of the PC (n = 11), from the olfactory tubercle (OT; n = 7), lateral amygdala (amy; n = 7), and l-EC (n = 11). As illustrated in Fig. 2A,B, runs of fast activity (arrows in Fig. 2A; see also expanded traces in Figs. 1 and 4–6) at circa 30–40 Hz were induced in all these regions within 4 min after the onset of 4AP arterial perfusion. FRs occurred asynchronously in the PCs of both hemispheres (rPC and coPC in Fig. 2). In all experiments, large-amplitude, all-or-none SLE that lasted 62.13 ± 46.9 s (average ± SD) emerged from these FRs (Fig. 2A). SLEs recurred every 1–2 min during 4AP perfusion. FRs were consistently induced at the onset of 4AP perfusion; sequences of FRs were also observed between two consecutive SLEs in the 38% of the experiments and at the end of an SLE (46% of the experiments).

To identify the olfactory structure(s) that initiated SLEs, we performed two types of experiments: (1) selective cortico-cortical disconnections between PC and adjacent areas and (2) local 4AP injections in different olfactory regions. As shown in Fig. 2A, we performed a cut that interrupted the connections between the rostral PC and the caudal PC and l-EC. As quantified in the plots in Fig. 2B,C, FRs and SLEs were abolished in regions caudal to the lesion. In addition, isolation of the OT from the PC with a longitudinal cut parallel and medial to LOT (see also Carriero et al., 2009) eliminated ictal activities in OT, but not in PC (n = 5; not shown).

Next, we locally applied by pressure-ejection small volumes of 4AP (2–5 mM; 3–5 pL) into different brain regions to test the ability of local networks to support FRs and SLE patterns. Local applications of 4AP in PC (n = 11; upper panel in Fig. 3) and OT (two of six) were able to induce the SLEs similar to those observed with arterial 4AP perfusion. FRs could be induced by local 4AP in OT (n = 6) and amygdala (four of six), but SLEs were never observed by applications in l-EC (n = 5; lower panel in Fig. 3) and amygdala (n = 6).

To further analyze the features of transition from FRs to SLEs we focused on the PC, where SLEs were most reliably induced. We identified reproducible SLE phases in all experiments (n = 25). FRs usually preceded SLE by 45.29 ± 27.67 s. The transition into SLE consistently occurred just during an FR (vertical arrow in Fig. 4A; see also Figs. 5 and 6). SLE onset was characterized by an abrupt positive transient deflection (termed phase I), followed by a period during which fast activity with a broader frequency range (20–60 Hz) was observed (phase II). The transition to phase III was consistently marked by the appearance of an

oscillation around 10 Hz (asterisk in Fig. 4A; see also Figs. 5B and 6), followed by the appearance of rhythmic population spikes that usually showed a progressive decremented rate. SLEs ended with a negative-going slow wave (arrowheads in Figs. 3, 4A and 5). In Fig. 4 and in the following figures, SLE phases are indicated by time bars with different gray shadings at the top of the traces. The frequency content in each SLE phase was analyzed by FFT and plots of the average frequency contents of the different phases are shown in Fig. 4B.

Intracellular activity in PC neurons during FRs and SLEs

We also analyzed the cellular substrates of SLEs by performing intracellular recordings from 21 neurons located in layers II (superficial layer) and III (deep layer) of PC during 15 experiments. Table 1 summarizes data on depth location and neurophysiological characteristics of the recorded neurons. During FRs and SLEs we observed two main patterns of neuronal activity in two separate populations of PC neurons. Type I cells (all positioned in layer II; n = 10; see insert microphotograph in Fig. 6) showed FR-associated membrane depolarization (ΔV_m = 15.0 ± 6.7 mV) coupled with fast oscillations at 30–40 Hz that could reach action potential firing threshold (Fig. 6A). During phase I at SLE onset, these cells showed a further, relatively rapid membrane depolarizing transient (ΔV_m from V_{rest} = 21.4 ± 7.4 mV) that was seldom associated with action potential firing (Figs. 5 and 6). Burst activity was never observed at SLE onset. During phase II, neuronal firing ceased in the majority of neurons (n = 7 of 9). During the transition between phases II and III (asterisks in Figs. 5 and 6), in coincidence with the extracellular 10 Hz activity, cells further depolarized (ΔV_m from V_{rest} = 34.9 ± 8.6 mV) and action potential firing was abolished (six of seven neurons). Membrane oscillations correlated with field potential oscillation were observed (n = 5). Phase III was associated with the maintenance of depolarizing plateau (ΔV_m from V_{rest} = 23.2 ± 4.9 mV) with neuronal firing that was synchronous with the extracellular population spiking (four of six, left traces in Figs. 5 and 6A). In addition, during SLE phase III, no bursting activity was observed. SLE recorded intracellularly in these neurons terminated with a rapid membrane potential repolarization that correlated with the slow negative wave in the extracellular trace (arrowhead in Fig. 5B). When the membrane potential was depolarized by a steady intracellular injection of positive current (n = 5), firing discharge during phase II was enhanced (n = 3; right traces in Fig. 5A,B), but dramatically decreased during phase III (right panels in Fig. 5A,B), presumably because of inactivation of voltage-dependent sodium channels (so-called depolarization block).

The second group of neurons (Table 1, type II; n = 11) was localized in layer III and showed a pattern characterized during FRs by small amplitude depolarizing deflections (ΔV_m = 9.01 ± 3.34 mV) without action potential firing or with isolated action potentials (Fig. 6B, upper panel). During phase I and phase II of SLEs, cells could further depolarize but did not fire action potentials (Fig. 6B). The transition between phases II and III in correspondence to 10 Hz (n = 7) featured membrane depolarization (ΔV_m from V_{rest} = 31.22 ± 5.7 mV), and firing was reached in four neurons (see cell in lower panel of Fig. 6B). In 8 of 10 neurons cell discharges were observed during the late part of phase III, when neurons repolarized at ΔV_m of 13.2 ± 7.5 mV (from V_{rest}; lower panel Fig. 6B). Figure 7 summarizes the averaged cell membrane potential values for the two groups of neurons (type I = circles; type II =

triangles) at resting condition, during FRs peak and the different phases of SLEs. One-way ANO-VA performed on the two groups of cells showed significant difference between the values of membrane depolarization during 10-Hz activity versus threshold values, FR peak, and SLE values in both layer II and layer III neurons (*$P < 0.05$). V_{rest} was significantly lower than all other mean values (**$P < 0.01$).

Discussion

Epileptiform discharges can be reproduced in in vitro preparations by application of proepileptic drugs. We have demonstrated that two region-specific epileptiform patterns are induced by 4AP in olfactory and in limbic areas of the in vitro isolated guinea pig whole brain (see also Carriero et al., 2010). The most likely action of this potassium channel blocker (Llinas et al., 1976) is facilitation of synaptic transmission due to a slowing of action potential repolarization in presynaptic terminals (Jankowska et al., 1977; Thesleff, 1980; Storm, 1987) at both excitatory and inhibitory synapses. This effect results in an amplification of synaptic network interactions and promotes the entrainment of network patterns that may ultimately sustain epileptiform discharges.

Within a few minutes after application of 4AP, olfactory cortices generated FRs and SLEs that (1) initiated within the PC and OT, (2) propagated to other olfactory–interconnected areas, such as the lateral amygdala and the l-EC, (3) did not propagate to hippocampus and m-EC, and (4) are originated by activity in neurons of the II layer of the PC. The pattern observed in this close-to-in vivo preparation is different from what most frequently observed in olfactory cortex slices of rats perfused with proconvulsive drugs. In slices, 4AP induced mainly interictal discharges (Hoffman & Haberly, 1993, 1996; Demir et al., 1999, 2001) or seizure-like events not dissimilar to those observed in other nonolfactory cortical areas maintained in vitro (Panuccio et al., 2012). Only a study by Galvan et al. performed on in vitro brain slices of guinea pig piriform cortex treated with 4AP showed seizure-like events comparable to FRs and SLEs described in the present study (e.g., Fig. 7 in Galvan et al., 1982). In this slice study, the initiation and development of seizure-like activity was highly variable and did show reproducible phases as described in the present report.

The olfactory and limbic regions are anatomically connected, with a strong rostrocaudal directionality mediated by associative fibers. PC massively projects to the l-EC and, with a minimal contingent, directly to the dentate gyrus of the hippocampus (Krettek & Price, 1978; Wilson & Steward, 1978; Luskin & Price, 1983; Room et al., 1984; Schwerdtfeger et al., 1990). When the LOT is stimulated, the projection from the rostral and caudal PCs sustains large amplitude polysynaptic responses in l-EC (Deadwyler et al., 1975; Kosel et al., 1981; Boeijinga & Van Groen, 1984; Van Groen et al., 1987; Chapman & Racine, 1997; Liu & Bilkey, 1997; Mouly et al., 1998; Biella & de Curtis, 2000; Gnatkovsky et al., 2004). From the l-EC, the olfactory-mediated input is massively relayed to the hippocampus via polysynaptic connections (Hjorth-Simonsen & Jeune, 1972; Leung et al., 1995; Canning & Leung, 1997; Biella & de Curtis, 2000). We demonstrated that the output projection of the hippocampus proper is differently conveyed into the medial and lateral EC in the guinea pig (Gnatkovsky et al., 2004). The m-EC receives a double input in both deep and superficial layers that sustains a reentrant entorhinal-hippocampal-entorhinal close-loop propagation

(Uva & de Curtis, 2005). Unlike the m-EC, the l-EC lacks the CA1-subicular input to deep layers and shows only a weak activation of superficial layers when the hippocampal output is activated (Gnatkovsky et al., 2004; Uva & de Curtis, 2005; Gnatkovsky & de Curtis, 2006). These data supported the conclusion that l-EC and m-EC represent two segregated and parallel input pathways that process olfactory and neocortical inputs, respectively, transfer their input to the hippocampus, and differently receive and process the hippocampal output (reviewed by Sewards & Sewards, 2003).

Region-specific, independent patterns isolated in the olfactory and the hippocampal-parahippocampal regions were already reported in the isolated guinea pig brain preparation following different pharmacologic manipulations. Arterial perfusion with bicuculline- or picrotoxin-induced seizure events localized exclusively to limbic structures, whereas large amplitude interictal spikes were recorded in the PC and in related olfactory areas (Librizzi & de Curtis, 2003). Moreover, when the cholinergic agonist, carbachol, was arterially perfused in this preparation, fast activities in the beta-gamma range were observed in both m-EC and hippocampus, but not in l-EC and in olfactory areas (van der Linden et al., 1999; Dickson et al., 2000). These findings further support the idea that region-specific synchronous patterns are commonly found in the brain and confirm that olfactory and limbic cortices are functionally segregated, even though they are anatomically connected. This connectivity pattern is consistent with the observed segregation of independent epileptiform activities in the olfactory area (inclusive of the l-EC) and in limbic areas. Propagation of seizure events from the limbic to the olfactory areas could be forced when seizure activity in the limbic region was recurring (Uva et al., 2005) and when interictal spike patterns were inactivated in the olfactory cortex (Librizzi & de Curtis, 2003).

As for bicuculline-induced epileptiform activity, 4AP application produced consistent events that were characterized at onset and during progression in olfactory and limbic regions. Epileptiform events induced by 4AP in m-EC-hippocampal area (defined as the limbic region) start with spikes (and not FRs) followed by seizures characterized by the sequential activation of fast activity at 20–30 Hz, followed by irregular spiking and bursting discharges (Carriero et al., 2010) generated bilaterally and synchronously. Unlike limbic seizures, SLEs in the olfactory system are independently generated in the two hemispheres and arise from an FR. No epileptiform population spikes were observed in the olfactory areas ahead of an SLE. SLE proceeded with a prolonged and sustained phase of low amplitude fast activity of broad frequency range (10–60 Hz) that lasted several tens of seconds and terminated with a sequence of rhythmic population spikes. Interestingly, and as a further difference in comparison to limbic seizures induced by 4AP, no population burst activity was observed during SLEs in olfactory regions recorded with extracellular electrodes. Consistent with this finding, action potential bursts were never recorded during SLEs in PC neurons. The initiation of an SLE was associated, indeed, with a slow depolarization of the membrane potential that did not correlate with intense neuronal firing, either bursting or tonic. SLE progression (phases II and III) in PC was characterized by progressive firing block and recovery of rhythmic single spike discharges; also in these phases neuronal spike clusters recognizable as bursts were never observed.

Neuronal firing was progressively depressed during phase II and blocked at the transition between phases II and III, and the block was prolonged when neurons were artificially depolarized by intracellular injection of a positive current during SLE. We propose that action potential depression at the transition between phase II/III is mediated by a depolarization block of neuronal firing, as suggested by the depolarization of neurons above or around spike threshold during SLE. The observed abolition of action potential firing is possibly due to voltage-dependent inactivation of sodium conductances (Bezanilla & Armstrong, 1974).

The depolarization occurring in deep cell population, which does not reach firing threshold during phases I and II, is significantly different in respect to the values measured for superficial cells displaying less negative membrane potential during FRs and SLE phases. Moreover the depolarization associated with the 10 Hz activity is significantly higher in both populations compared to the other phases considered.

The two patterns of intracellular activity were associated with a different layering of cells in the PC. We observed that type 1 cells were located in the superficial layer of the PC, which is densely populated with pyramidal and semilunar cells, whereas the type 2 cells were positioned in the deep layer of PC, which is constituted by pyramidal cells and multipolar cells (Neville & Haberly, 2004). The higher density of cells in layer II with a restricted extracellular space could favor the ephaptic interactions among cells and affect excitability changes in the extracellular environment. On the contrary, PC layer III is characterized by a lower density of cells, by a lower density of excitatory pyramidal cells compared to layer II, and relatively higher number of inhibitory multipolar cells, suggesting a proportional increase in the inhibitory networks. The anatomic difference between the two groups of cells could explain at least partially, the different behavior of the two neuronal groups. Moreover, we did not observe a difference in the intrinsic electrophysiological parameters between type 1 and type 2 cells. A different distribution of voltage-sensitive potassium channels, target of the 4AP, in superficial versus deep PC layers should also be taken into account. A study published on this topic (Weiser et al., 1994) describes the different expression of Shaw-related K^+ channels messenger RNAs (mRNAs) in the rat PC, with the highest expression of $K_V3.2$ mRNAs in the most superficial part of the cell layer, even though a detailed quantification was not performed.

The absence of intense firing in principal neurons at the onset of 4AP-induced SLEs suggests that activity in these neurons is not enhanced at the very onset of hyperexcitable events that resemble a seizure. A similar conclusion was also reached by studying seizure initiation in the transient disinhibition model of acute limbic seizures induced by brief bicuculline applications in the isolated guinea pig brain (Gnatkovsky et al., 2008; de Curtis & Gnatkovsky, 2009; Trombin et al., 2011). In this model, the onset of seizures in the m-EC correlated with an increase in interneuronal firing and was associated with a blockade of spike generation in principal neurons. Seizure progression in this model was supported by changes in extracellular potassium (Gnatkovsky et al., 2008; Trombin et al., 2011). A depression of principal cell activity coupled with an increase in interneuronal firing was also reported in hippocampal slices (Ziburkus et al., 2006; Fujiwara-Tsukamoto et al., 2007) and in the immature isolated whole hippocampus (Derchansky et al., 2008). Interestingly, a

reduction in single unit firing has been reported in human focal seizures analyzed with microelectrode recordings during diagnostic presurgical intracranial exploration (Truccolo et al., 2011). Whether an increase in interneuronal activity was also the cause of the depression of firing in PC superficial cells at SLE onset is not clear.

Conclusions

The present study demonstrates that the convulsant 4AP induces a region-specific epileptiform pattern in olfactory cortices. This epileptiform activity is independent on and different from seizure activity simultaneously recorded in other brain areas, such as in the limbic cortices. These findings validate the hypothesis that brain areas strongly interconnected can generate synchronous and autonomous epileptiform patterns (both interictal and ictal). The generation and propagation of epileptiform discharges within a hard-wired network is consistent with the recent proposal that extends the concept of focal epilepsy to a dysfunction of a brain network (Berg et al., 2010). Moreover, the identification of selective networks able to generate independent acute epileptiform events supports the definition of the olfactory region and the limbic region as independent brain systems potentially predisposed to develop region-specific forms of epilepsy.

Supplementary Material

Refer to Web version on PubMed Central for supplementary material.

Acknowledgments

The work was supported by an ERANET-NEURON grant *2-p imaging*, by the Ministero della Sanità (Ricerca Corrente 2011–2012), by Cariplo Foundation (2010–2012), and by the Canadian Institutes of Health Research (CIHR grants 8109 and 102710).

References

Avanzini G, Manganotti P, Meletti S, Moshe SL, Panzica F, Wolf P, Capovilla G. The system epilepsies: a pathophysiological hypothesis. Epilepsia. 2012; 53:771–778. [PubMed: 22533642]

Avoli M, Perreault P. A GABAergic depolarizing potential in the hippocampus disclosed by the convulsant 4-aminopyridine. Brain Res. 1987; 400:191–195. [PubMed: 3028566]

Avoli M, D'Antuono M, Louvel J, Kohling R, Biagini G, Pumain R, D'Arcangelo G, Tancredi V. Network and pharmacological mechanisms leading to epileptiform synchronization in the limbic system in vitro. Prog Neurobiol. 2002; 68:167–207. [PubMed: 12450487]

Berg AT, Berkovic SF, Brodie MJ, Buchhalter J, Cross JH, van Emde Boas W, Engel J, French J, Glauser TA, Mathern GW, Moshe SL, Nordli D, Plouin P, Scheffer IE. Revised terminology and concepts for organization of seizures and epilepsies: report of the ILAE Commission on Classification and Terminology, 2005–2009. Epilepsia. 2010; 51:676–685. [PubMed: 20196795]

Bezanilla F, Armstrong CM. Gating currents of the sodium channels: three ways to block them. Science. 1974; 183:753–754. [PubMed: 4821243]

Biella G, de Curtis M. Olfactory inputs activate the medial entorhinal cortex via the hippocampus. J Neurophysiol. 2000; 83:1924–1931. [PubMed: 10758103]

Biella GR, Gnatkovsky V, Takashima I, Kajiwara R, Iijima T, de Curtis M. Olfactory input to the parahippocampal region of the isolated guinea pig brain reveals weak entorhinal-to-perirhinal interactions. Eur J Neurosci. 2003; 18:95–101. [PubMed: 12859341]

Boeijinga PH, Van Groen T. Inputs from the olfactory bulb and olfactory cortex to the entorhinal cortex in the cat. Exp Brain Res. 1984; 57:40–48. [PubMed: 6519229]

Canning KJ, Leung LS. Lateral entorhinal, perirhinal and amygdala-entorhinal transition projections to hippocampal CA1 or dentate gyrus in the rat: a current source density study. Hippocampus. 1997; 7:643–655. [PubMed: 9443060]

Carriero G, Uva L, Gnatkovsky V, de Curtis M. Distribution of the olfactory fiber input into the olfactory tubercle of the in vitro isolated guinea pig brain. J Neurophysiol. 2009; 101:1613–1619. [PubMed: 18922946]

Carriero G, Uva L, Gnatkovsky V, Avoli M, de Curtis M. Independent epileptiform discharge patterns in the olfactory and limbic areas of the in vitro isolated Guinea pig brain during 4-aminopyridine treatment. J Neurophysiol. 2010; 103:2728–2736. [PubMed: 20220076]

Chapman AC, Racine RJ. Converging inputs to the entorhinal cortex from the piriform cortex and medial septum: facilitation and current source density analysis. J Neurophysiol. 1997; 78:2602–2615. [PubMed: 9356410]

Danober L, Deransart C, Depaulis A, Vergnes M, Marescaux C. Pathophysiological mechanisms of genetic absence epilepsy in the rat. Prog Neurobiol. 1998; 55:27–57. [PubMed: 9602499]

de Curtis M, Gnatkovsky V. Reevaluating the mechanisms of focal ictogenesis: the role of low-voltage fast activity. Epilepsia. 2009; 50:2514–2525. [PubMed: 19674056]

de Curtis M, Biella G, Forti M, Panzica F. Multifocal spontaneous epileptic activity induced by restricted bicuculline ejection in the piriform cortex of the isolated guinea pig brain. J Neurophysiol. 1994; 71:2463–2475. [PubMed: 7931528]

de Curtis M, Biella G, Buccellati C, Folco G. Simultaneous investigation of the neuronal and vascular compartments in the guinea pig brain isolated in vitro. Brain Res Protoc. 1998; 3:221–228.

Deadwyler SA, West JR, Cotman CW, Lynch G. Physiological studies of the reciprocal connections between the hippocampus and entorhinal cortex. Exp Neurol. 1975; 49:35–57. [PubMed: 171171]

Demir R, Haberly LB, Jackson MB. Sustained and accelerating activity at two discrete sites generate epileptiform discharges in slices of piriform cortex. J Neurosci. 1999; 19:1294–1306. [PubMed: 9952407]

Demir R, Haberly LB, Jackson MB. Epileptiform discharges with in-vivo-like features in slices of rat piriform cortex with longitudinal association fibers. J Neurophysiol. 2001; 86:2445–2460. [PubMed: 11698534]

Derchansky M, Jahromi SS, Mamani M, Shin DS, Sik A, Carlen PL. Transition to seizures in the isolated immature mouse hippocampus: a switch from dominant phasic inhibition to dominant phasic excitation. J Physiol. 2008; 586:477–494. [PubMed: 17991696]

Dickson CT, Biella G, de Curtis M. Evidence for spatial modules mediated by temporal synchronisation of carbachol induced gamma rhythm in medial entorhinal cortex. J Neurosci. 2000; 20:7846–7854. [PubMed: 11027250]

Fujiwara-Tsukamoto Y, Isomura Y, Imanishi M, Fukai T, Takada M. Distinct types of ionic modulation of GABA actions in pyramidal cells and interneurons during electrical induction of hippocampal seizure-like network activity. Eur J Neurosci. 2007; 25:2713–2725. [PubMed: 17459104]

Galvan M, Grafe P, ten Bruggencate G. Convulsant actions of 4-aminopyridine on the guinea-pig olfactory cortex slice. Brain Res. 1982; 241:75–86. [PubMed: 7104708]

Gloor P, Fariello RG. Generalized epilepsy: some of its cellular mechanisms differ from those of focal epilepsy. Trends Neurosci. 1988; 11:63–68. [PubMed: 2465601]

Gnatkovsky V, de Curtis M. Hippocampus-mediated activation of superficial and deep layer neurons in the medial entorhinal cortex of the isolated guinea pig brain. J Neurosci. 2006; 26:873–881. [PubMed: 16421307]

Gnatkovsky V, Uva L, de Curtis M. Topographic distribution of direct and hippocampus- mediated entorhinal cortex activity evoked by olfactory tract stimulation. Eur J Neurosci. 2004; 20:1897–1905. [PubMed: 15380011]

Gnatkovsky V, Librizzi L, Trombin F, de Curtis M. Fast activity at seizure onset is mediated by inhibitory circuits in the entorhinal cortex in vitro. Ann Neurol. 2008; 64:674–686. [PubMed: 19107991]

Hjorth-Simonsen A, Jeune B. Origin and termination of the hippocampal perforant path in the rat studied by silver impregnation. J Comp Neurol. 1972; 174:591–606.

Hoffman WH, Haberly LB. Role of synaptic excitation in the generation of bursting-induced epileptiform potentials in the endopiriform nucleus and piriform cortex. J Neurophysiol. 1993; 70:2550–2561. [PubMed: 8120598]

Hoffman WH, Haberly LB. Kindling-induced epileptiform potentials in piriform cortex slices originate in the underlying endopiriform nucleus. J Neurophysiol. 1996; 76:1430–1438. [PubMed: 8890264]

Jankowska E, Lundberg A, Rudomin P, Sykova E. Effects of 4-aminopyridine on transmission in excitatory and inhibitory synapses in the spinal cord. Brain Res. 1977; 136:387–392. [PubMed: 200308]

Khalilov I, Holmes GL, Ben-Ari Y. In vitro formation of a secondary epileptogenic mirror focus by interhippocampal propagation of seizures. Nat Neurosci. 2003; 6:1079–1085. [PubMed: 14502289]

Kosel KC, Van Hoesen GW, West JR. Olfactory bulb projection to the parahippocampal area of the rat. J Comp Neurol. 1981; 198:467–482. [PubMed: 7240454]

Krettek JE, Price JL. Amygdaloid projections to subcortical structures within the basal forebrain and brainstem in the rat and cat. J Comp Neurol. 1978; 178:225–254. [PubMed: 627625]

Leresche N, Lambert RC, Errington AC, Crunelli V. From sleep spindles of natural sleep to spike and wave discharges of typical absence seizures: is the hypothesis still valid? Pflugers Arch. 2012; 463:201–212. [PubMed: 21861061]

Leung LS, Roth L, Canning KJ. Entorhinal inputs to the hippocampal CA1 and dentate gyrus in the rat: a current source density analysis. J Neurophysiol. 1995; 73:2392–2403. [PubMed: 7666147]

Librizzi L, de Curtis M. Epileptiform ictal discharges are prevented by periodic interictal spiking in the olfactory cortex. Ann Neurol. 2003; 53:382–389. [PubMed: 12601706]

Liu P, Bilkey DK. Parallel involvement of perirhinal and lateral entorhinal cortex in the polysynaptic activation of hippocampus by olfactory inputs. Hippocampus. 1997; 7:296–306. [PubMed: 9228527]

Llinas R, Walton K, Bohr V. Synaptic transmission in squid giant synapse after potassium conductance blockage with external 3- and 4-aminopyridine. Biophys J. 1976; 16:83–86. [PubMed: 1244891]

Luhmann HJ, Dzhala VI, Ben-Ari Y. Generation and propagation of 4-AP-induced epileptiform activity in neonatal intact limbic structures in vitro. Eur J Neurosci. 2000; 12:2757–2768. [PubMed: 10971618]

Luskin MB, Price JL. The laminar distribution of intracortical fibers originating in the olfactory cortex of the rat. J Comp Neurol. 1983; 216:292–302. [PubMed: 6863605]

McIntyre DC, Gilby KL. Mapping seizure pathways in the temporal lobe. Epilepsia. 2008; 49(Suppl 3):23–30.

Mouly AM, Litaudon P, Chabaud P, Ravel N, Gervais R. Spatiotemporal distribution of a late synchronized activity in olfactory pathways following stimulation of the olfactory bulb in rats. Eur J Neurosci. 1998; 10:1128–1135. [PubMed: 9753181]

Muhlethaler M, de Curtis M, Walton K, Llinas R. The isolated and perfused brain of the guinea-pig in vitro. Eur J Neurosci. 1993; 5:915–926. [PubMed: 8281302]

Neville, KR., Haberly, L. Olfactory cortex. In: Shepherd, GM., editor. The synaptic organization of the brain. Oxford University Press; New York: 2004. p. 415-454.

Panuccio G, Sanchez G, Levesque M, Salami P, de Curtis M, Avoli M. On the ictogenic properties of the piriform cortex in vitro. Epilepsia. 2012; 53:459–468. [PubMed: 22372627]

Perreault P, Avoli M. Physiology and pharmacology of epileptiform activity induced by 4-aminopyridine in rat hippocampal slices. J Neurophysiol. 1991; 65:771–785. [PubMed: 1675671]

Piredda S, Gale K. A crucial epileptogenic site in the deep prepiriform cortex. Nature. 1985; 317:623–625. [PubMed: 4058572]

Room P, Groenewegen HJ, Lohman AH. Inputs from the olfactory bulb and olfactory cortex to the entorhinal cortex in the cat. I. Anatomical observations. Exp Brain Res. 1984; 56:488–496. [PubMed: 6499975]

Satou M, Mori K, Tazawa Y, Takagi SF. Monosynaptic and disynaptic activation of pyriform cortex neurons by synchronous lateral olfactory tract volleys in the rabbit. Exp Neurol. 1983; 81:571–585. [PubMed: 6884469]

Schwerdtfeger WK, Buhl EH, Germroth P. Disynaptic olfactory input to the hippocampus mediated by stellate cells in the entorhinal cortex. J Comp Neurol. 1990; 292:163–177. [PubMed: 2319007]

Sewards TV, Sewards MA. Input and output stations of the entorhinal cortex: superficial vs. deep layers or lateral vs. medial divisions? Brain Res Brain Res Rev. 2003; 42:243–251. [PubMed: 12791442]

Storm JF. Action potential repolarization and a fast-hyperpolarization in rat hippocampal pyramidal cells. J Physiol. 1987; 385:733–759. [PubMed: 2443676]

Thesleff S. Aminopyridines and synaptic transmission. Neuroscience. 1980; 5:1413–1419. [PubMed: 6250099]

Trombin F, Gnatkovsky V, de Curtis M. Changes in action potential features during focal seizure discharges in the entorhinal cortex of the in vitro isolated guinea pig brain. J Neurophysiol. 2011; 106:1411–1423. [PubMed: 21676935]

Truccolo W, Donoghue JA, Hochberg LR, Eskandar EN, Madsen JR, Anderson WS, Brown EN, Halgren E, Cash SS. Single-neuron dynamics in human focal epilepsy. Nat Neurosci. 2011; 14:635–641. [PubMed: 21441925]

Uva L, de Curtis M. Polysynaptic olfactory pathway to the ipsi- and contralateral entorhinal cortex mediated via the hippocampus. Neuroscience. 2005; 130:249–258. [PubMed: 15561441]

Uva L, Librizzi L, Wendling F, de Curtis M. Propagation dynamics of epileptiform activity acutely induced by bicuculline in the hippocampal-parahippocampal region of the isolated Guinea pig brain. Epilepsia. 2005; 46:1914–1925. [PubMed: 16393157]

van der Linden S, de Curtis M, Panzica F. Carbachol induces fast oscillations in the medial but not in the later entorhinal cortex of the isolated guinea pig brain. J Neurophysiol. 1999; 82:2441–2450. [PubMed: 10561417]

Van Groen T, Lopes da Silva FH, Wadman WJ. Synaptic organization of olfactory inputs and local circuits in the entorhinal cortex, a current-source density analysis in the cat. Exp Brain Res. 1987; 67:502–509. [PubMed: 3653312]

van Luijtelaar G, Sitnikova E. Global and focal aspects of absence epilepsy: the contribution of genetic models. Neurosci Biobehav Rev. 2006; 30:983–1003. [PubMed: 16725200]

Weiser M, Vega-Saenz de Miera E, Kentros C, Moreno H, Franzen L, Hillman D, Baker H, Rudy B. Differential expression of Shaw-related K+ channels in the rat central nervous system. J Neurosci. 1994; 14:949–972. [PubMed: 8120636]

Wilson RC, Steward O. Polysynaptic activation of the dentate gyrus of the hippocampal formation: an olfactory input via the lateral entorhinal cortex. Exp Brain Res. 1978; 33:523–534. [PubMed: 215436]

Ziburkus J, Cressman JR, Barreto E, Schiff SJ. Interneuron and pyramidal cell interplay during in vitro seizure-like events. J Neurophysiol. 2006; 95:3948–3954. [PubMed: 16554499]

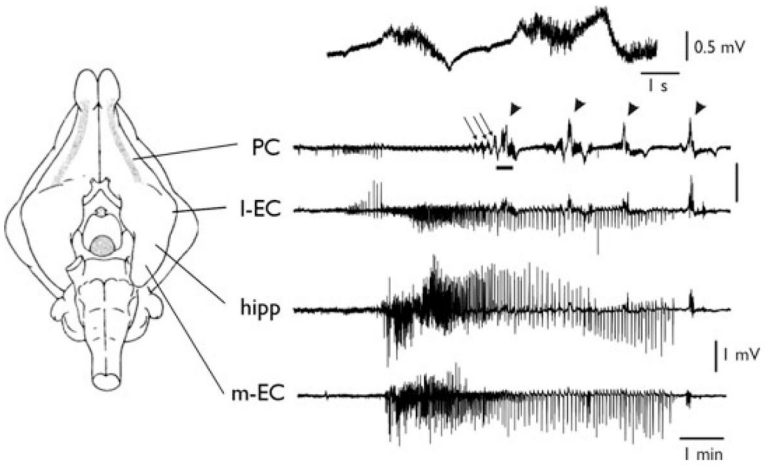

Figure 1.

Independent epileptiform patterns induced by arterial perfusion of 4AP in the olfactory and limbic systems. Extracellular recordings from piriform cortex (PC), lateral entorhinal cortex (l-EC), CA1 region of the hippocampus (hipp), and medial entorhinal cortex (m-EC), after arterial perfusion of 50 μM 4AP in the in vitro isolated guinea pig brain. Electrode position is illustrated in the scheme on the left. Runs of fast activity and seizure-like events are marked by the arrows and arrowheads, respectively. The upper trace illustrates an expansion of the PC recording underlined by the thick tract showing details of FRs.

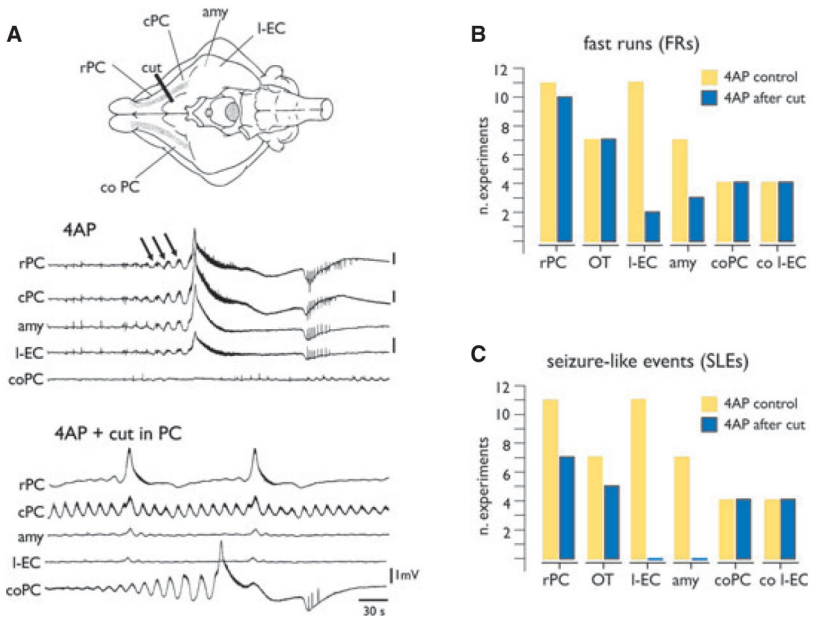

Figure 2.

Distribution of 4AP-induced seizure-like events (SLE) in the olfactory system. (**A**) Recordings from two different sites in the PC (rostral, rPC and caudal, cPC), in the lateral amygdala (amy), the lateral EC (l-EC) of the right hemisphere and from PC of the contralateral hemisphere (coPC) during arterial perfusion of 50 μM 4AP. As shown in the traces of the upper panel, runs of fast activity (FR; arrows) and SLEs were recorded. Electrode position is shown in the scheme on top. Epileptiform activity is asynchronous between the hemispheres. A scalpel cut (cut in the schematic drawing) was performed between rPC and cPC. The effect of the cut on the distribution of FRs and SLEs is illustrated in the lower panel in (**A–C**): Quantification of the effect of the cut between rPC and cPC on the distribution of FRs (**B**) and SLEs (**C**) in olfactory and limbic structures. OT, olfactory tubercle; co l-EC, contralateral l-EC. The number of experiments is shown on the Y axis. *Epilepsia* © ILAE

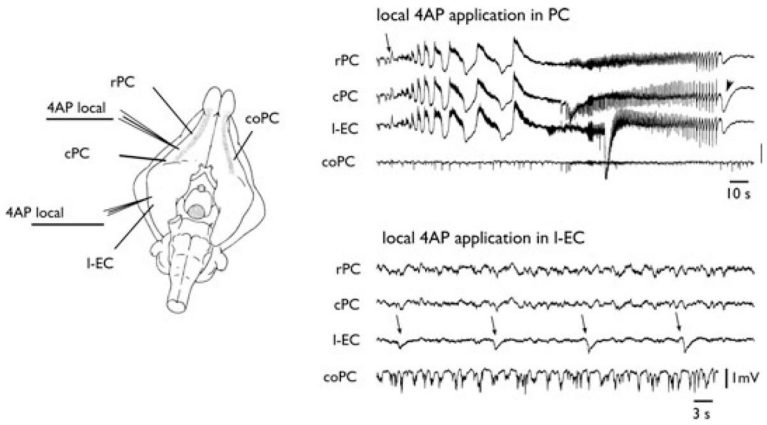

Figure 3.

Local application of 4AP in the PC induces FR and SLE. The left panel illustrates the position of the recording electrodes and the site of the ejection pipettes filled with 2 mM 4AP. On the right, the effects of 100-msec local applications of 4AP (arrows) in the PC (upper panel) and in the l-EC (lower panel) are shown. FRs and SLEs are induced by local 4AP injection in PC. The arrowheads point to the negative deflection at the end of the SLE. *Epilepsia* © ILAE

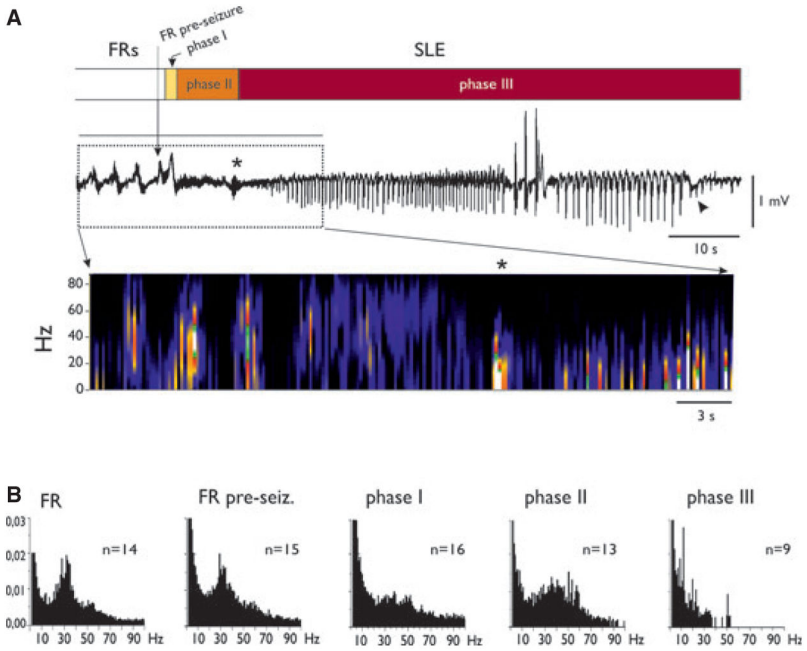

Figure 4.

Characterization of reproducible SLE phases induced in the PC by arterial perfusion of 4AP. (**A**) Extracellular recordings performed during an SLE. FRs and SLE phases are illustrated in the upper bar by different intensities of gray shading. The ~10 Hz activity at the transition between phase II and phase III is marked by the asterisk. The arrowhead points to the negative deflection at the end of the SLE. In the lower part of the panel the spectrogram of the SLE is illustrated. (**B**) Averaged fast Fourier transform plots of the recordings in different phases of the epileptiform event. Power frequency content during FRs, FRs just before an SLE (FR pre-SLE), and during phases I, II, and III of SLEs are illustrated. *Epilepsia* © ILAE

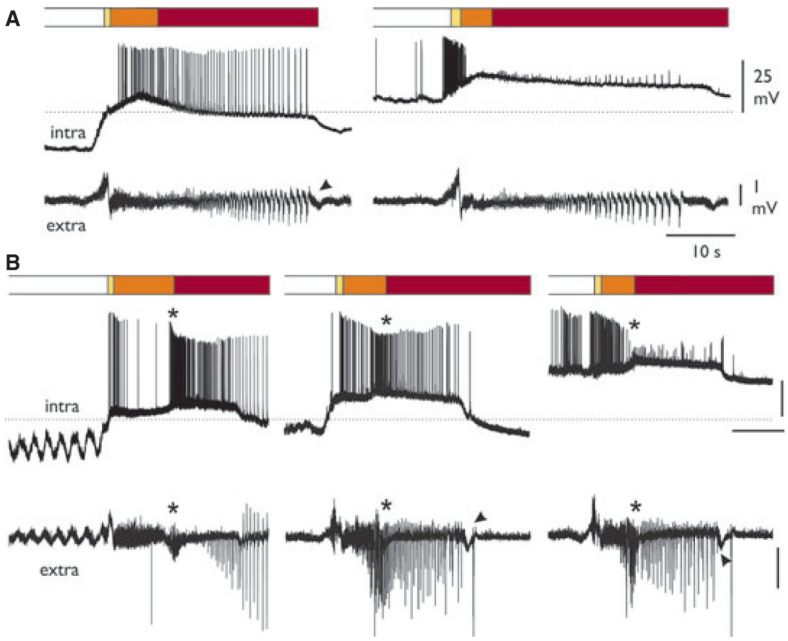

Figure 5.

Intracellular recordings during 4AP-induced SLEs in PC layer II neurons. SLE phases are indicated by gray shadings in the upper bars (see also Fig. 4). Simultaneous intracellular (upper traces) and extracellular recordings (lower traces) are shown. (**A**) Intracellular recordings performed in the same layer II cell at two different membrane potentials, set by intracellular injection of either hyperpolarizing (left intra trace) or depolarizing (right intra trace) current. Resting membrane potential (dotted line) is −62 mV. (**B**) Intracellular recordings performed at three different membrane potential polarizations in another layer II PC neuron. Resting membrane potential (dotted line) is −56 mV. Asterisks mark the ~10 Hz activity at the transition between phases II and III. The arrowheads point to the negative deflection at the end of the SLE.

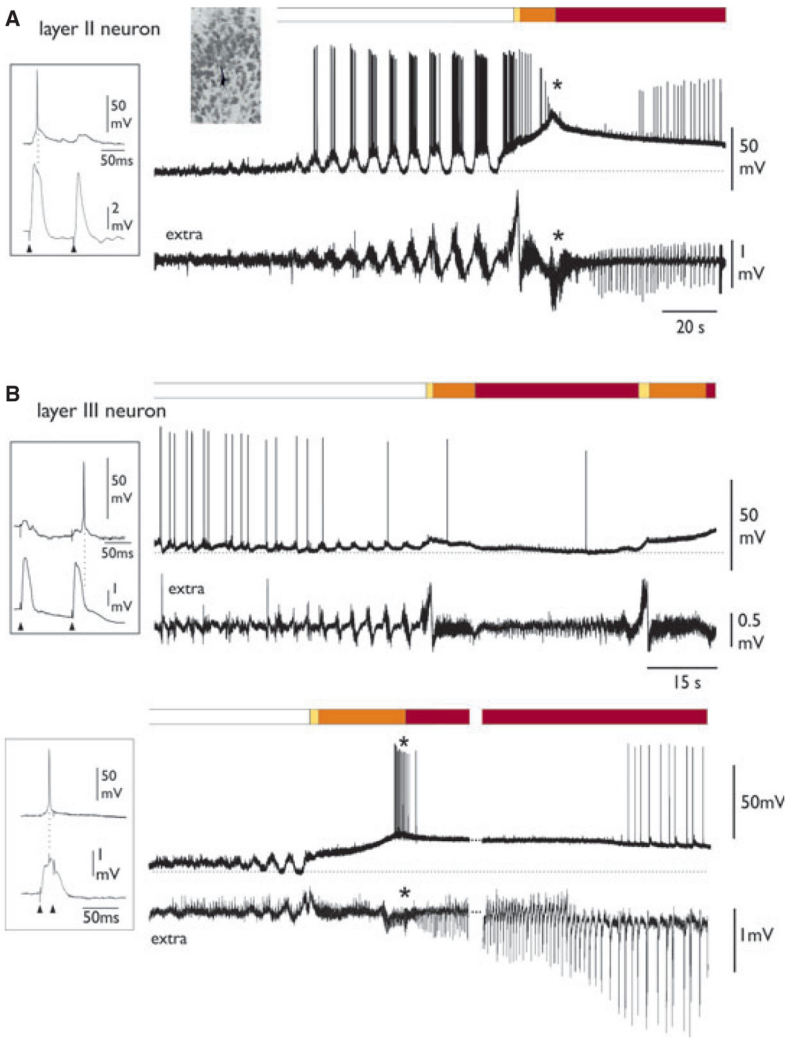

Figure 6.

Different intracellular patterns in layer II and III neurons during 4AP-induced SLEs. The phases of SLE are illustrated in the upper bars. (**A**) Typical intracellular SLE pattern of a layer II PC neuron, recorded simultaneously to the extracellular activity (lower trace). The asterisk marks the transition between phases II and III. Resting membrane potential (dotted line) was −70 mV. (**B**) Intracellular SLE pattern of two different deep layer (III) PC neurons, with simultaneous recording of the extracellular activity (lower trace). Resting membrane potentials (dotted lines) were −63 and −67 for the upper and lower neurons, respectively. *Epilepsia* © ILAE

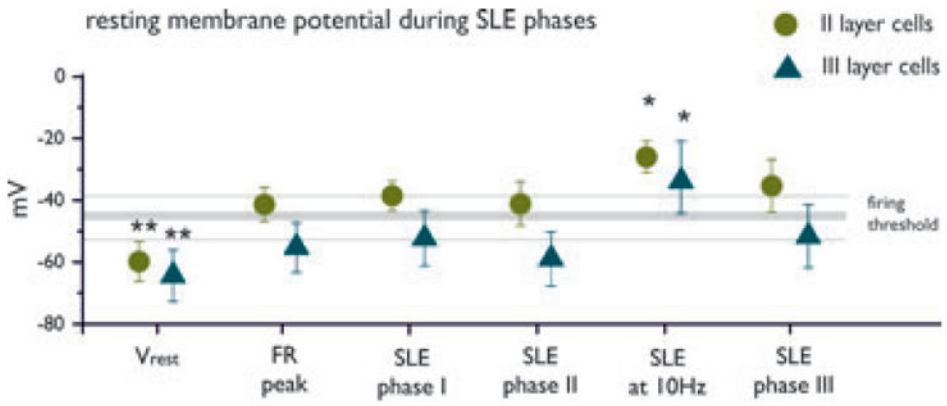

Figure 7.

Membrane potential values during FRs and SLEs. Averaged membrane potential values (±SD) during resting (V_{rest}, before 4AP perfusion), fast runs (FRs), phase I, phase II, the transition between phase II and III characterized by 10 Hz activity and phase III of SLEs are reported. The range (±SD) of the firing threshold is also reported. Mean values obtained from neurons located in layers II and III are represented by filled circles and triangles, respectively. ANOVA showed statistically significant differences of membrane potential values against all other phases of FR-SLE (FR peak, phases I, II, and III) in both cell populations (*$P < 0.05$; **$P < 0.01$).

Epilepsia © ILAE

Table 1

Summary of the depth location and neurophysiological characteristics of the recorded neurons

Cell type	Localization	RMP	Input resistance	Firing threshold	AP amplitude
Type I (n = 10)	II layer (n = 10)	−59.8 ± 6.4 mV	38.6 ± 15.6 MΩ	−42.2 ± 6.5 mV	63.8 ± 10.4 mV
Type II (n = 11)	III layer (n = 11)	−63.6 ± 8.7 mV	36.4 ± 13.4 MΩ	−44.5 ± 6.4 mV	64.4 ± 11.1 mV

RMP, resting membrane potential; AP, action potential.